

2018

Finite Element Analysis of a Guideway for Automated Transit Networks

Issac Gendler

Follow this and additional works at: <https://scholarworks.sjsu.edu/mcnair>



Part of the [Mechanical Engineering Commons](#)

Recommended Citation

Gendler, Issac (2018) "Finite Element Analysis of a Guideway for Automated Transit Networks," *McNair Research Journal SJSU*: Vol. 14 , Article 8.

<https://doi.org/10.31979/mrj.2018.1408> <https://scholarworks.sjsu.edu/mcnair/vol14/iss1/8>

This Article is brought to you for free and open access by SJSU ScholarWorks. It has been accepted for inclusion in McNair Research Journal SJSU by an authorized editor of SJSU ScholarWorks. For more information, please contact scholarworks@sjsu.edu.



Isaac Gendler

Major:
Mechanical Engineering

Mentor: **Dr. Burford J.
Furman**

Finite Element Analysis of a
Guideway for Automated
Transit Networks

Biography

*Isaac Gendler is dedicated to using his bachelor's degree in Mechanical Engineering to make an impact in the world of sustainable infrastructure systems and make science more accessible to everyone. In this pursuit, he has performed research at both SJSU and Lawrence Berkeley National Laboratory, worked with the March for Science – San Francisco, writes a daily science blog (<https://isaacscienceblog.wordpress.com/>) and cofounded a club called **NEED: The Network for Environmental and Energy Development**, an organization dedicated to bringing a sustainability research platform to campus. For his future career, Isaac wants to enter a doctorate program in engineering specializing in control systems for sustainability purposes.*

Finite Element Analysis of a Guideway for Automated Transit Networks

Abstract

An asymmetric beam currently being utilized in a solar powered automated transit system was analyzed for its deflections, stresses, and angle of twist. Finite element analysis (FEA) with ANSYS was used in conjunction with hand calculations from beam theory to determine the response of the guideway to loading anticipated in normal operation. An iterative approach was used for modeling the system, where the geometry was taken from a simplified case and progressed in complexity until the original model was duplicated. After analysis, the deflections, stresses, and angles of twist were found to be within suitable ranges for a suspended transportation system.

1. Introduction

The structural performance of an asymmetric beam being used in a personal rapid transport system was computationally analyzed using Finite Element Analysis (FEA). FEA can be performed on a variety of structures (Sachdeva et. al 2017), such as personal rapid transit (PRT) systems. A PRT system uses podcars, which are automated driverless vehicles, to transport passengers on a guideway (Furman et. al 2014). FEA is a modern software tool that is integral in the design process to help ensure that parts and structures will not fail under anticipated loading conditions. Since these guideways will be supporting a number of podcars, the analysis has been done for the worst-case scenario.

One such system is being developed at San Jose State University, known as the Spartan Superway (Furman 2016) (Fig 2.1). The Spartan Superway employs an elevated guideway (a beam which upholds the podcar) developed by Beamways Inc. (U.S. Patent No. 8,807,043, 2014) to serve as the framework for mobility. Before implementation, the structural elements of the asymmetric beam need detailed FEA to be

completed. After analysis, it was found that the deformations, stresses, and twisting were in safe ranges for public transportation.

Figure 1.1: The Spartan Superway system. Full-scale model of a section of the guideway, cross section used for analysis shown.



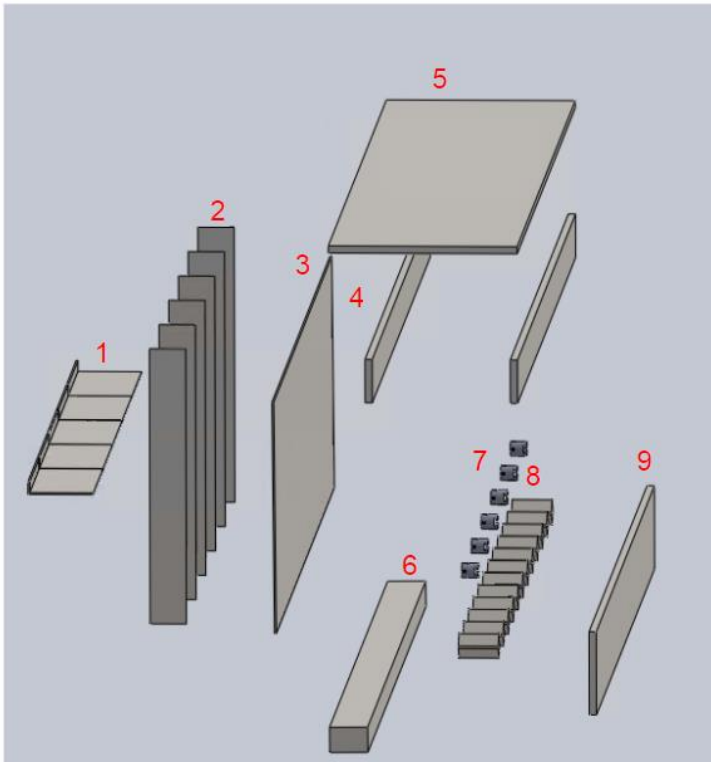
2. Set up

2.1 The Guideway

The guideway currently being used by the Spartan Superway was developed by Bengt Gustafsson of Beamways PRT systems (2014, 2016). The guideway (Fig. 2.2) is composed of eight modular three meter long sections, each having 12 pegs, six insulators, six ribs, five debucklers, one side plate, two vertical bars, one lower stringer, one rail, and one ceiling (Gustafsson 2014). The dimensions are 520mm wide by 1000mm high by 24000mm long, and the modulus of elasticity for steel is 200000 N/mm^2 .

Due to its asymmetrical cross section, analytical methods are insufficient to accurately predict deflections, stresses, and twist.

Figure 2.1: Exploded view of the guideway. Parts in increasing order from left to right: (1) debucklers, (2) ribs, (3) side plate, (4) vertical bar, (5) ceiling (6) lower stringer (7) insulator (8) stud (9) rail.



2.2 Loading

The guideway must be designed to withstand its own worst-case loading scenario. Such a scenario entails the guideway experiencing a heavy wind force while podcar vehicles are at maximum capacity, stationary, and stacked nose to tail. Numerical analysis (Appendix) establishes that the bogie would be experiencing a relatively large lateral wind force of 1981 N on its wheels to the upper side wall and 3130 N to the outer lower side of the running surface flange where the switching

wheels engage. The remaining wind pressure of 306 Pascals would act directly on the outer part of the upper guide wheel running surface flange, and the weight of the bogie wheels would induce 5396 N of force every 1.5 meters (Fig 2.3) (Gustafsson 2016).

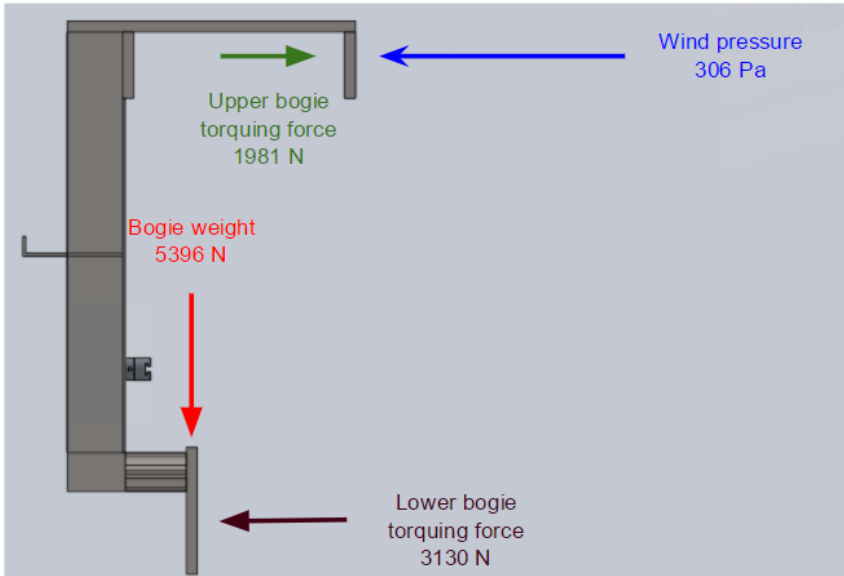


Figure 2.2: Outline of the force assumptions. Each arrow represents a force with magnitude.

3. Methodology

3.1 Finite Element Analysis (FEA)

FEA is a modern computer simulation tool that uses numerical methods to solve engineering problems that have no existing analytic solution and/or if the cost of experimental testing is too prohibitive. FEA works by discretizing a Computer Aided Design (CAD) geometry into a multitude of discrete “elements” to be connected at “nodes” (geometric edges) to create a “mesh.” The object’s behavior is then subject to “governing equations” and “boundary conditions.” Governing equations describe and relate how the physics of a model interact within its own structure (Bhavikatti 2014) to solve for field variables (the dependent

variables of interests) while the boundary conditions specify the values of the boundary field variables, such as the supports for a spring.

To illustrate this concept, Hooke's law, $F = kx$ is a governing equation that describes how a spring system works, while the force would be the boundary variable. In this system, the governing equations will be those applied to static cases (such as stress is equal to force divided by area, $\sigma = \frac{F}{A}$) while the field variables would be the deformation and stresses, and the boundary conditions would be the supports used.

FEA goes through three stages:

- (i) The Pre-processing phase, in which the material properties, geometry, meshing (elements and nodes), loads, and boundary conditions are specified.
- (ii) The Solution phase, in which all of the variables are interrelated to solve the field variables.
- (iii) The Post-processing phase, in which the values for the solution will be displayed.

3.2 ANSYS

To perform FEA, a software package must be used. One such package is known as ANSYS. ANSYS has been used by many different parties, ranging from academics researching structural engineering (Al-Sherrawi et. al 2014, Hua, X. G, et al. 2007) to engineers working on offshore wind turbines (Sahroni 2015), and even the yacht team of Team New Zealand (ANSYS 2013). After post processing, the selected field variables (such as deformation or stresses) are displayed visually on the elements, with each color corresponding to a range of values, all of which can be changed at the user's discretion (Fig 3.2).

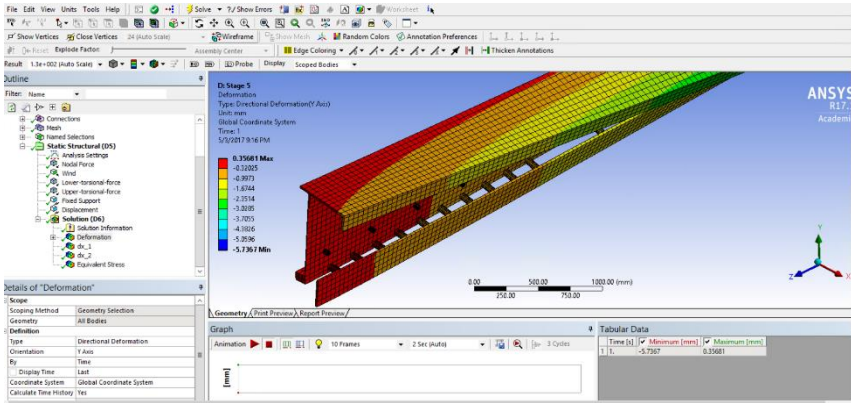


Figure 3.1: View of ANSYS. Display of deformation post processing values. Each element color corresponds to a range of possible values, as dictated by the bar to the left of the object. The minimum value of the color depends on the lowest value of its box on the bar, while the maximum value on its highest.

3.3 Iteration Based Approach

Since FEA must be used carefully on models in which no known analytic solution is present (as verification of any results can only be done with approximations), the project was divided into five iterations. The first iteration began with a simple loading situation on a beam approximated by a rectangular solid bar geometry whose dimensions reflected the parameters of the Beamway guideway profile. For the next three iterations, the geometry was given refined characteristics to produce a greater resemblance to the guideway, leading up to the fifth and final iteration, in which the original model was used. To illustrate the advantage, think of a sculptor and a stone tablet. Before the final image can be realized, the artist must start with a block that contains sufficient parameters, and must then carve said block, incrementing the design until the work has been perfected (Fig. 3.3). For all iterations, a mesh size of one node for every 50 mm was applied.

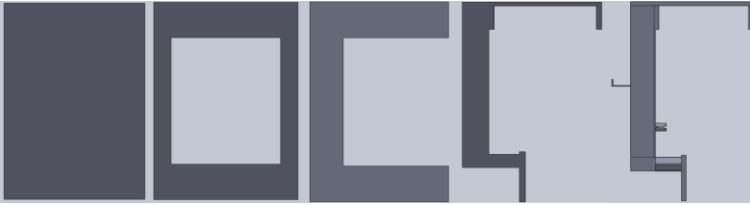


Figure 3.2: Cross sections used in successive iterations of analysis. From left to right: Solid rectangular profile, Hollow rectangular profile, C profile, G cross section, final profile.

4. Analysis Iterations

4.1 Iteration 1: Solid Rectangular Profile

The first iteration is a bar with a solid rectangular cross section. The dimensions of the profile were based off the extremities of the original model, 520mmx1000mmx24000mm. Simple supports (constraining the front end to one translational degree of freedom and the back end to two) were used for the simulation and placed at the bottom edge of the profile and all the bogie forces were combined into a single central load of 80940 N which was used to simplify simulation. The wind and torque forces were not simulated since the geometry was deemed too simple. To verify the results from ANSYS, the linear deflection in the y-axis at the midspan can be predicted using the equation (Fig 4.1).

$$d = \frac{5PL^3}{384EI} \quad (1)$$

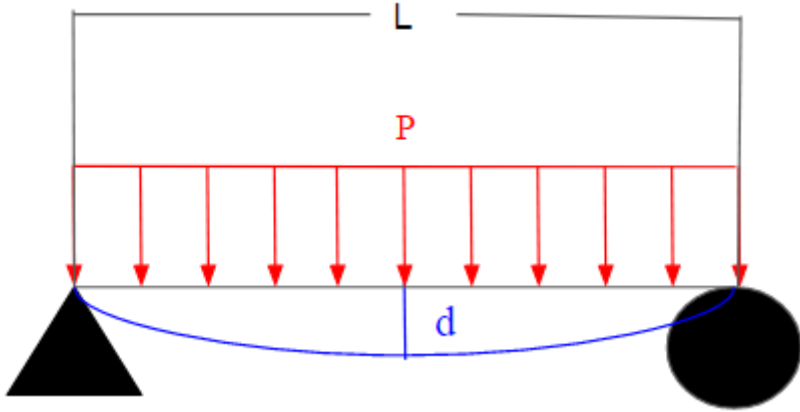


Figure 4.1: Diagram of loading. The linear load P acts over the entire length L to produce a deformation d .

In this system, P is taken to be the linear pressure loading ($\frac{80940N}{24000mm} \rightarrow 3.37 \text{ N/mm}$), L to be the length (24000 mm), E to be the modulus of elasticity (200000 N/mm), and I to be the area moment of inertia (being equal to $\frac{b^3}{12} \rightarrow \frac{520mm*(1000mm)^3}{12} \rightarrow 4.33 * 10^{10} \text{ mm}^4$). Since the force in ANSYS was applied to a rectangular face, it was treated as a linear pressure for modeling. After hand calculations, the deflection results came out to be equal to 1.68 mm . Through ANSYS calculation, the final result came out to be 1.69 mm , within 0.6% of the prediction. The von Mises stress for the system at midspan can be calculated with the equation:

$$\sigma = \frac{PL^2}{8S} \quad (2)$$

with S being the section modulus ($\frac{b^2}{6} \rightarrow \frac{520mm*1000mm^2}{6} \rightarrow 86666666.67 \text{ mm}^3$), coming out to be 2.8 MPa . With an ANSYS simulation, the stresses at midspan were analyzed to be 2.795 MPa , a difference from the analytic solution of around 1.8% . No twisting was observed.

4.2 Iteration 2: Hollow Rectangular Profile

Since the beam is not perfectly solid and contains gaps, a logical step would be to incorporate a hole into the second iteration. The dimensions for said hole were based upon the area encapsulated between the top vertical bars and the lower horizontal bar, due to its easy to find and symmetric nature. The profile for the iteration was then modified accordingly, giving it a moment of inertia $I = I_{Outer} - I_{inner} = \frac{520mm*(1000mm)^3}{12} - \frac{395mm*(640mm)^3}{12} = 34.7 * 10^{10} mm^4$ and a section modulus $S = \frac{b_{larger}(\square_{larger})^3 - b_{smaller}(\square_{smaller})^3}{6 \square_{larger}} = \frac{520mm(1000mm)^3 - 390mm(640mm)^3}{6(1000mm)} = 6.94 * 10^7 mm^3$. Material properties were kept the same. Using equation (1) for deformation and equation (2) for stresses, 2.10 MPa and 3.5 MPa were predicted respectively. The vertical deformation was 2.13 mm, which was within 1.4% of the predicted value. The von Mises stress near the midpoint was 3.48 MPa with a 0.57% error.

4.3 Iteration 3: The C Profile

Since the Beamways beam profile does not contain a central hole, the next iteration should reflect that. As such, the gap was moved to the right to transform the beam into a “C” geometry (Fig 3.3). The previous loading and support scheme was retained. The new moment of inertia around the x-axis can be calculated using the equation:

$$I_{xx} = \frac{(\square - t_1)^3 t_2}{12} + 2 \left[\frac{b t_1^3}{12} + b t_1 \left(\frac{\square - t_1}{2} \right)^2 \right] \quad (3)$$

With:

- being the height (1000mm)
- b being the base (520mm)
- t₁ being the thickness of the top and bottom pieces (180mm)
- t₂ being the thickness of the centerpiece of the C beam (125 mm)

All of this results in a moment of inertia equivalent to around $2.82 * 10^{10} \text{ mm}^4$, while the section modulus S is equivalent to $\frac{I}{\square/2} \rightarrow \frac{2.82 * 10^{10} \text{ mm}^4}{1000 \text{ mm}/2} \rightarrow 5.64 * 10^7 \text{ mm}^3$. After inserting these values into equations (1) and (2), answers of 2.10 mm and 0.04 MPa were arrived at respectively. ANSYS simulations reported around 2.49 mm (Fig 4.2) for deflection and 3.0 MPa for stresses (Fig. 4.3), resulting in error values of 18.6% and 7400% respectively.

Since the beam was not perfectly symmetric around the y-axis and the force was not placed at the shear center, twisting had occurred in the model. As such, it should be studied. The angle of twist for a particular geometry can be found using the equation:

$$\theta = \frac{dx_2 - dx_1}{L} \quad (4)$$

Where dx_2 is the displacement of the top element of a linear geometry from the x-axis, dx_1 is the displacement of the bottom element of a linear geometry from the x-axis, and L (1000 mm in this case) is the distance between them. (Fig. 4.3) Data was collected from the ANSYS model through analyzing the x-axis displacement from each node corresponding to dx_2 and dx_1 across the the z-axis path, plugging it into equation (4), and then graphing. From this, it can be observed that a maximum twist of $5.76 * 10^{-4}$ radians occurs at midspan w , forming a parabolic structure (Fig. 4.4). Since there was a slightly different number of elements between dx_1 and dx_2 , the data for the first 10 results is uncorrelated and may be ignored.

Since the loading was not going through the shear center, analytic solutions were available. Instead, ANSYS simulations were used in place.

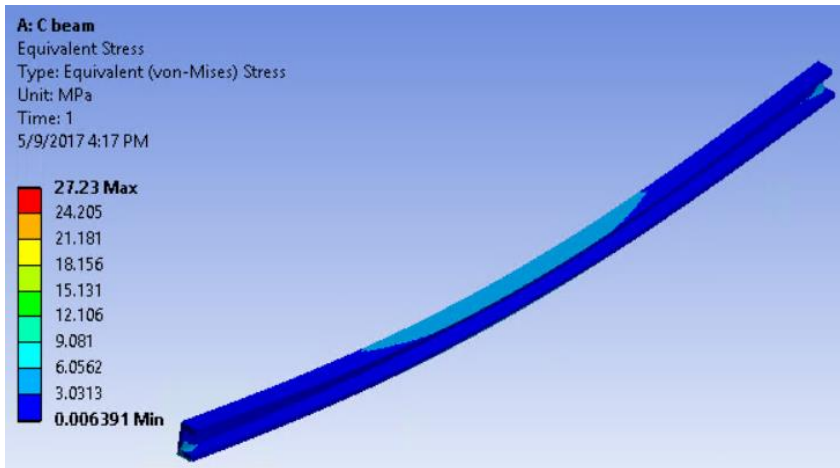


Figure 4.2: Iteration 3 deflection results. Deflections are curved due to twisting.

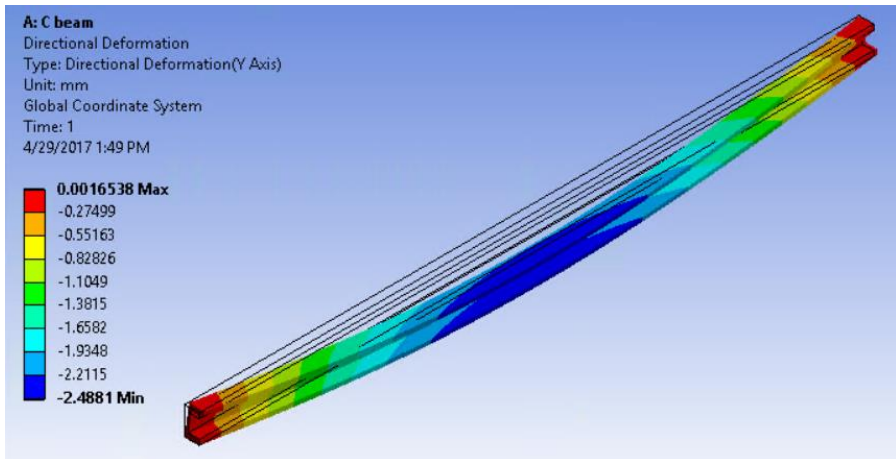


Figure 4.3: Iteration 3 stress results.

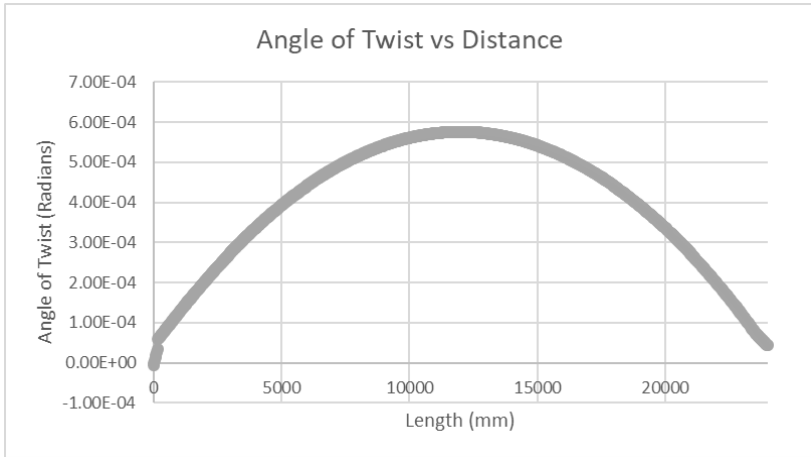


Figure 4.4: Measure of twist around axis Z for iteration 3. Max twisting occurs near the center of the beam length. The discontinuity near the beginning is a result of a different number of elements between the two paths.

4.4 Iteration 4: The G Profile

The next iteration was to make the geometry similar to an idealized version of the beamway profile. The new profile was made to be a uniform version of the original guideway. The lower edges of the profile were chosen for simple supports. Because the geometry of this model had a high similarity to the original version, the loading schematic was modified to more accurately resemble the initial parameters: 1981 N of the force through its wheels to the left chamber wall, 3130N to the outer lower railing, and a bogie weight of 5396 N every 1.5 meters with a wind force of 306 Pascals on the top railing (Fig 4.5). After ANSYS analysis, the deformation came out to be around 0.73 mm, (Fig 4.6), the stresses 0.008 MPa at mid center (Fig 4.7), and the max twisting to be $3.34 * 10^{-4}$ radians, occurring near midspan (L was equal to 757 mm for three significant figures rounding) (Fig 4.8).

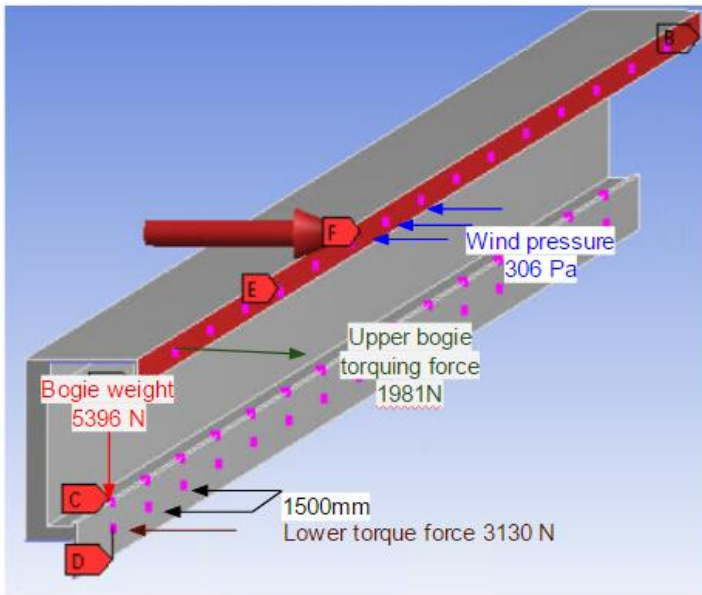


Figure 4.5: Force placement layout for iteration 4. Forces repeat every 1500 mm.

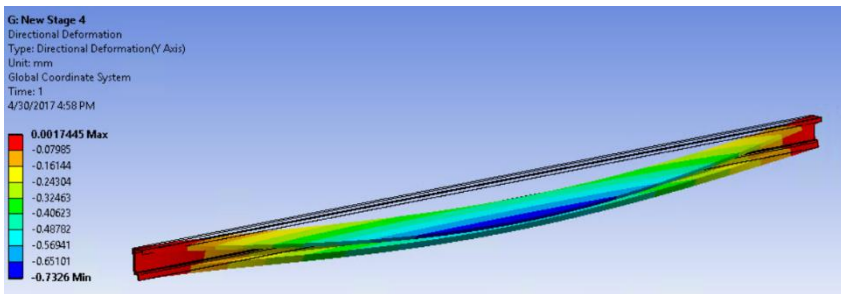


Figure 4.6: Iteration 4 deflection results. Max deflection takes place at the upper surface flange at midspan.

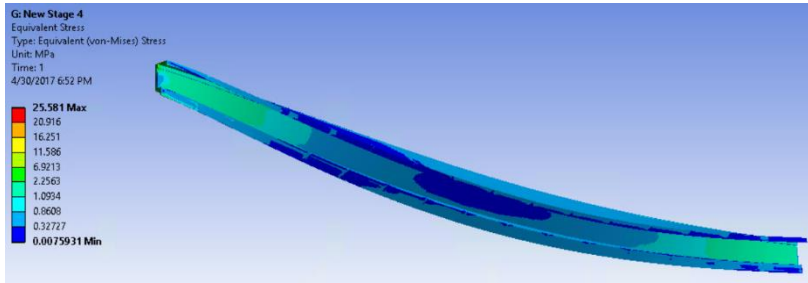


Figure 4.7: Iteration 4 stress results.



Figure 4.8: Iteration 4 twist. Measure of twist around axis Z for section 4. Maximum angle of twist occurs near midspan. Near the end the results become uncorrelated.

4.5 Iteration 5: The Final Profile

For the fifth and final iteration, the geometry was fashioned to replicate the original model, with the exception that every 12th peg in the model had to be removed due to compilation issues. The loadings and support structure were duplicated from iteration four. The maximum deflection was near 4.35 mm (Fig 4.9) while the largest stresses were around 2.53 MPa (Fig 4.10). The maximum angle of twist was $1.00 * 10^{-2}$ radians (Fig 4.11).

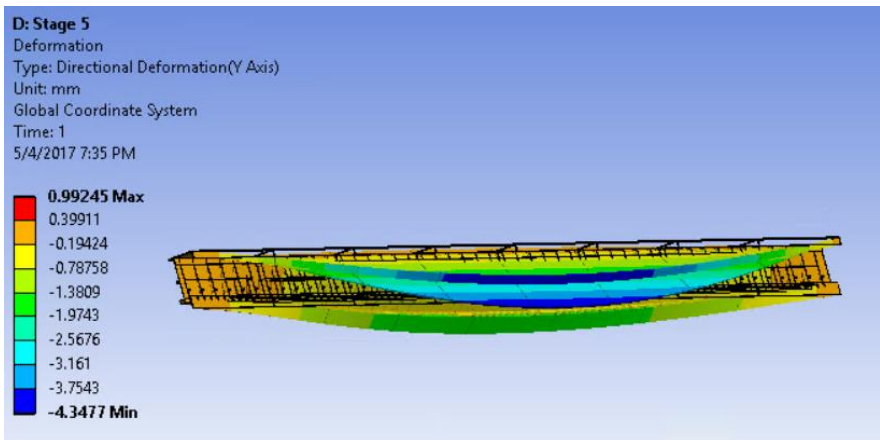


Figure 4.9: Iteration 5 deflection results. Max deflection takes place at the upper surface flange at midspan.

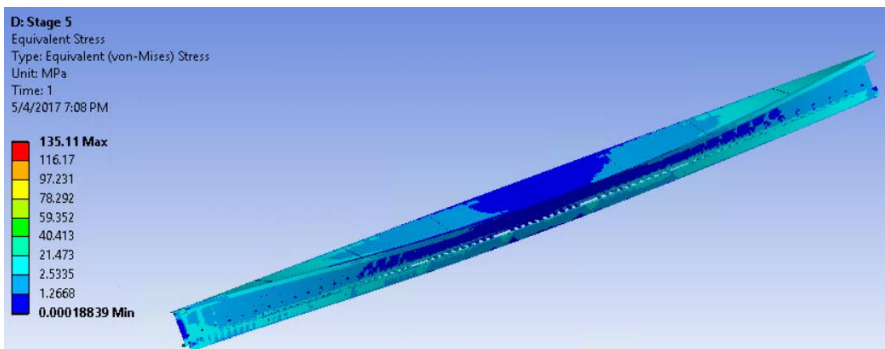


Figure 4.10: Iteration 5 stress results. Stress is non-uniform due to twisting.

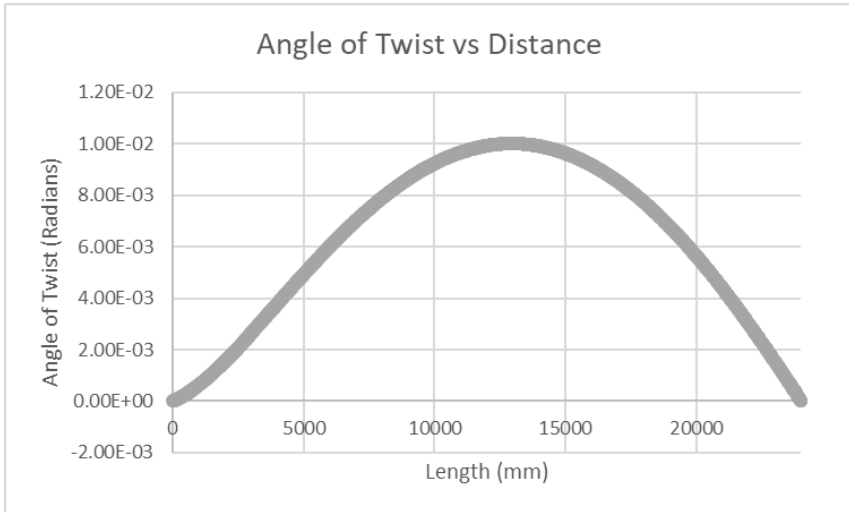


Figure 4.11: Iteration 5 graph of twisting. Measure of twist around axis Z for iteration 5. dx_1 and dx_2 elements had perfect correlation.

5. Conclusion

After simulations were completed, the deformations of the guideway from the anticipated loads have been found to be safe for public use. The deflection values obtained were far smaller than ones found in real world bridges, such as Scotland’s Forth Road Bridge (Roberts et. al 2012), and the stress values were far smaller than those of the Huangpu Bridge in Guangzhou, China (Wang et. al 2014).

Acknowledgements

Gilles Eggenspieler, Khody Afkhami, and ANSYS Inc. provided the software, tutorials, and training needed to perform this project. Eduardo Chan shared his expertise with finite-element analysis to assist with this project. Burford Furman suggested this research project, assisted with the research process, and provided priceless feedback. Ron Swenson and Kurt McMullin advised on the iteration process. Mohannad Husain Al-Sherrawi of the University of Baghdad and Chirag Sachdeva of PEC University of Technology assisted with calculating the necessary moment of inertias for parts of the iterations.

7. Appendix: Derivation of Bogie Torsional Loads

The wind pressure point is located at 1.5 meters below the bottom of the guideway (Gustafsson 2016).

$$\sum F_x \square = -F_{Lower} + F_{\square ig \square er} + F_{Wind \ on \ Bogie} = 0$$

$$\sum M \square = -x_1 F_{Lower} * + x_2 F_{\square ig \square er} = 0$$

Solving for the moment will give us:

$$\longrightarrow F_{lower \square} = \frac{x_2}{x_1} F_{\square ig \square er}$$

From the CAD model, x_1 was found to be 1.39 meters and x_2 was found to be 2.19 meters (assuming that the forces would be applied at the center of their respected areas).

$$\longrightarrow F_{Lower} = 1.58 F_{\square ig \square er}$$

The linear force on the bogie would be equal to 766N/m (Gustafsson 2016) and multiplying by 1.5 meters would yield 1149N. Combining this value with the aforementioned moment equation, one would arrive at:

$$\begin{aligned} 1.58 F_{\square ig \square er} + F_{\square ig \square er} &= -1149 \text{ N} \\ F_{\square ig \square er} &= 1981 \text{ N} \end{aligned}$$

And through back substitution, one would logically find that:

$$F_{\square ig \square er} = 3130 \text{ N}$$

References

- ANSYS Inc. (2013). *Case study: Computer simulation improves America's cup yacht*. Retrieved from: <https://www.ansys.com/-/media/ansys/corporate/resourcelibrary/casestudy/etnz-case-study.pdf>
- Bhavikatti, S. S. (2014). *Finite element analysis*. New Delhi: New Age International Pvt.

- Furman, B., Fabian, L., Ellis, S., Muller, P., & Swenson, R., (2014). *Automated transit networks (ATN): A review of the state of the industry and prospects for the future* (No. CA-MTI-14-1227). Retrieved from: <http://transweb.sjsu.edu/project/1227.html>
- Furman, B. J. (2016). The Spartan Superway: A solar-powered automated transportation network. American Solar Energy Society National Conference 2016, San Francisco.
- Gustafsson, B. (2014). *Patent Identifier No. 8,807,043*. Washington, DC: U.S. Patent and Trademark Office.
- Gustafsson, B. (2016). *Beamways track geometry*. Linköping: Beamways.
- Hua, X. G., Chen, Z. Q., Ni, Y. Q., & Ko, J. M. (2007). Flutter analysis of long-span bridges using ANSYS. *Wind and Structures, 10*(1), 61-82.
- Mohannad H. Al-Sherrawi, S.M. (2014). The effective width in composite steel concrete beams at ultimate loads. *University of Baghdad Engineering Journal, 20*(8).
- Roberts, G. W., Brown, C. J., Meng, X., Ogunidipe, O., Atkins, C., & Colford, B. (2012). Deflection and frequency monitoring of the forth road bridge, Scotland, by GPS. *Proceedings of the Institution of Civil Engineers - Bridge Engineering, 165*(2), 105-123. doi:10.1680/bren.9.00022
- Sachdeva, C., Miglan, J., Padhee, S.S. (2017). Study for effectiveness of idealized theory for Fuselage section through finite element analysis. *58th AIAA/ASME/ASCE/AHS/ASC Structures, Structural Dynamics and Materials Conference*. doi: <https://arc.aiaa.org/doi/book/10.2514/MSDM17>
- Sahroni, T. R. (2015). Modeling and simulation of offshore wind power platform for 5 MW baseline NREL turbine. *The Scientific World Journal*. doi: <http://dx.doi.org/10.1155/2015/819384>
- Wang, W., & Liang, J. (2014) Stress measuring and monitoring for main tower of Guangzhou Pearl River HuangPu Bridge. *Proceedings Volume 7375, ICEM 2008: International Conference on Experimental Mechanics 2008; 73754G*. doi:10.1117/12.839306